Advances in Continuous and Discrete Models

RESEARCH Open Access

The impact of lifting COVID-19 restrictions on influenza transmission across countries

Wenyu Du[1], Zhenghui Feng[2] and Yi Zhao[2*]

*Correspondence:
zhao.yi@hit.edu.cn
[2]School of Science, Harbin Institute of Technology, Shenzhen, 518055, China
Full list of author information is available at the end of the article

Abstract

Background: The COVID-19 pandemic has had a profound global impact. This study aims to assess the impact of lifting COVID-19 restrictions on the transmission dynamics of influenza across various countries, investigating how the timing of these policy changes influences influenza outbreaks and public health responses.

Methods: We used daily COVID-19 case data and weekly influenza case data to estimate the effective reproduction number (R_t) for both diseases before and after reopening. Additionally, we conducted counterfactual analyzes using Seasonal ARIMA models to predict influenza positivity rates.

Results: Lifting COVID-19 restrictions led to COVID-19 transmission increase, but postponed the outbreak of influenza. Countries were categorized based on the timing of easing restrictions relative to the influenza season: near the influenza peak (China, UK), outside the season (USA, South Africa), and without clear seasonality (Singapore, Indonesia). For the first group, reopening delayed the influenza peak; for the second, the impact on peak duration was minimal; for the third, lifting restrictions led to a rapid but controlled outbreak. Specifically in China, the influenza peak was delayed by 10 weeks and the peak infection rate was 10.4% higher following the reopening.

Conclusion: The findings underscore the complex interplay between COVID-19 and influenza transmission and highlight the divergent impacts of reopening measures on infectious diseases, indicating that the timing of policy measures is crucial for mitigating influenza outbreaks. Then insights gained can enhance resource allocation and offer a new perspective for public health.

Keywords: Influenza Transmission; Effective Reproduction Number; Counterfactual Scenario; Lifting COVID-19 Restrictions

1 Background

Since December 2019, the coronavirus disease (COVID-19) has rapidly disseminated worldwide, which is distinguished by its rapid transmission, extensive infectivity, and formidable challenges in terms of prevention and control, thereby imposing substantial burdens on the public healthcare systems of diverse nations [1–5]. Due to the lack of effective pharmaceutical interventions specifically targeting the novel virus, various nations adopted non-pharmaceutical interventions (NPIs) to mitigate the transmission of

COVID-19 [6–9]. Influenza is a seasonal respiratory infectious disease that poses a significant risk to public health worldwide. Albeit the vaccinations, the disease continues to present a substantial burden, contributing to annual cases and mortality on a global scale [10, 11].

Due to the emergence of various COVID-19 variants, characterized by reduced pathogenicity and enhanced transmissibility, alongside significant economic repercussions and public waning patience, governments worldwide adopted strategies of easing epidemic control measures. This action involves aiming for coexistence with COVID-19 and pursuing herd immunity through a combination of vaccination campaigns and natural infection. Subsequent to the easing of epidemic control measures, there has been a notable rise in both the incidence and fatality rates of viral infections [12–15]. However, it is notable that the variants exhibit a lower-case fatality rate compared to earlier strains. Studying the dynamics of epidemic propagation is an effective approach to controlling the spread of infectious diseases. The COVID-19 pandemic has had unexpected impacts on respiratory diseases [16–21], with some being suppressed while others experience resurgence during off-seasons. Among these, the influence of the pandemic on influenza has been particularly notable. Due to the control measures implemented for COVID-19, the transmission of influenza viruses has significantly decreased, indicating that public health interventions have effectively suppressed the spread of influenza [22]. Research suggests that the SARS-CoV-2 virus and influenza viruses may interact in certain contexts, such as through competition for host resources or by influencing immune responses [23]. These dynamic changes have added complexity to the medical response to the pandemic.

However, there has been insufficient attention to the scale and severity of post-lockdown outbreaks in various countries. This may be attributed to a relaxation in public attitudes towards COVID-19 and inadequate reporting [24]. We specifically focus on the impact of the timing of epidemic restrictions lifting on influenza transmission, a perspective that has been less explored in previous studies on complex networks. Additionally, our research is based on real-world data regarding influenza and COVID-19 infection rates, allowing for concrete empirical analysis, whereas complex network models often rely on assumptions and simulations [25–27]. The impact of ending NPIs on COVID-19 and influenza remains uncertain, despite the economic recovery observed after lifting restrictions. Therefore, characterizing the transmissibility of COVID-19 and influenza following the lifting of restrictions requires a comprehensive analysis. Given the public health imperative in light of these circumstances, Burki et al. concluded that the variant after lifting restrictions is roughly 60% more transmissible than the variant during the lockdown period in England [28]. On the other hand, the magnitude of behavioral responses following sudden repeals of lockdown measures may be smaller than anticipated by policymakers [29]. A difference-in-differences design and linear fixed-effects regressions were developed to estimate the effect of lifting COVID-19 restrictions. The analysis yielded a conclusion that lifting restrictions has the potential to engender a surge in demand for certain primary healthcare services [30].

Given the disparities in geography, climate, and public health policies across different countries, the transmission patterns of SARS-CoV-2 and influenza exhibit distinct characteristics in various national contexts. To capture these divergent propagation dynamics and their reciprocal interactions, a data-driven model to estimate the effective reproduction number (R_t) of COVID-19 and influenza after lifting COVID-19 restrictions has been

introduced as a key metric. Furthermore, counterfactual analyzes have been conducted to explore the impact of reopening measures on influenza, both in the absence of the COVID-19 pandemic and under the continued presence of the SARS-CoV-2 virus. In this study, countries are classified into three representative groups based on the alignment between influenza transmission patterns and national reopening policies over time. This study is the first to employ a country grouping approach to compare the transmission dynamics of COVID-19 and influenza, thereby filling a gap in the existing literature. The selected countries are China, the United States, and Singapore. As for China, on January 23, 2020, Wuhan implemented a city-wide lockdown in response to the COVID-19 outbreak [31]. Subsequently, various provinces across China swiftly conducted NPIs to enforce strict disease control measures. As a result of these concerted efforts, the epidemic was effectively controlled, leading to the complete lifting of restrictions on December 8, 2022. The American government implemented NPIs starting on March 13, 2020, and the measures were then lifted on April 1, 2021. In April 2020, there was a sharp increase in COVID-19 cases among foreign workers residing in dormitories in Singapore, which prompted the Singaporean government to conduct a comprehensive nationwide lockdown policy [32]. After two months, the containment strategy transitioned to a "suppression strategy", which was subsequently implemented until April 26, 2022, when a complete lifting of restrictions occurred.

Timely evaluation of the transmission trends of COVID-19 and influenza is crucial for controlling pandemic disasters. Adopting an approach of grouping countries, this study examines the transmission dynamics of COVID-19 and influenza in each representative group. The findings highlight the varying impacts of reopening measures on the transmission dynamics of COVID-19 and influenza across different national contexts. After reopening, the transmission of infectious diseases is likely to rebound, leading to a rapid increase in cases and new outbreaks that put strain on healthcare systems. Thus, evaluating the effects of reopening on influenza transmission can yield valuable insights for resource allocation and the formulation of public health policies in the post-pandemic landscape. Integrating lessons learned about the indirect effects of COVID-19 policies on respiratory disease patterns can strengthen preparedness and resilience in the face of future public health emergencies. Our findings inform public health decision-making and the design of tailored intervention strategies to mitigate the burden of both emerging and recurrent infectious diseases.

2 Materials and methods

2.1 Source of data

Due to the varying timelines of lifting restriction measures across countries, this study revolves around the lifting restriction date as a reference point and focuses on the daily new infection data for a period of six months before and after the lifting. The data utilized in this study was sourced exclusively from official government websites of the respective countries. Regarding China, the influenza-like illness (ILI) surveillance data was publicly released by the National Influenza Surveillance Network in mainland China, covering the period from December 5, 2016, to June 18, 2023 [33]. For the US, the national sentinel surveillance data on ILI was obtained from the Centers for Disease Control and Prevention (CDC) website, covering the time range from March 13, 2017, to October 10, 2021 [34]. In the case of Singapore, the ILI data was retrieved from the Ministry of Health's official website (MOH), specifically spanning from February 6, 2017, to October 30, 2022 [35].

For the United Kingdom, the data about ILI was obtained from the UK Health Security Agency (UKHSA) website, with a period from July 19, 2021, to September 4, 2022 [36]. Lastly, the influenza data for South Africa and Indonesia were sourced from the Global Influenza Surveillance and Response System (GISRS) of the World Health Organization (WHO), encompassing the time range from March 23, 2020, to April 11, 2021, and from June 20, 2022, to July 9, 2023 [37]. Public health and clinical laboratories in each country report the total number of respiratory specimens tested for influenza and the number of individuals testing positive for the influenza virus to the government on a weekly basis. In the case of Singapore, the data provided includes the average daily number of patients seeking treatment in polyclinics for Acute Respiratory Infection (ARI) and the proportion of patients with ILI among polyclinic attendances for ARI. To obtain the weekly number of individuals testing positive for influenza virus, these two measures were multiplied together. We can estimate the number of daily influenza cases by multiplying the daily ILI counts by the proportion of ARI patients testing positive for influenza [38].

We also considered the daily new COVID-19 cases from the publicly available data set on the website *Our World in Data* [39]. It is widely acknowledged that the SARS-CoV-2 virus responsible for COVID-19 undergoes genetic changes over time, resulting in the emergence of new variants. Due to variations in the timing of lifting restrictions across different countries, the study periods differ, thereby contributing to variations in the prevalence of specific variants within the respective study periods. Specifically, within the corresponding study periods, the Delta variant (B.1.617.2) was prevalent in the US, while the Omicron variant (B.1.1.529) was identified in China, Singapore, the UK and Indonesia, and the Beta variant (B.1.351) was observed in South Africa.

2.2 Estimation of the reproduction number (R_t)

The reproduction number, denoted as R_t, is a fundamental epidemiological metric used to quantify the average number of secondary cases generated by a typical case of an infectious disease in a completely susceptible population [40]. It characterizes the transmission dynamics of a disease within a population.

We built a Bayesian frame described in the previous studies [41, 42] to calculate the effective reproduction number. It is assumed that individuals exhibit an infectivity profile after infection characterized by a probability distribution w_s. R_t can be defined as the quotient of the number of new infections generated at time step t, I_t, and the total infectiousness of individuals who are infected at time t, Λ_t, the cumulative infection incidence up to time step $t-1$, weighted by the infectivity function w_s, with $\Lambda_t = \sum_{s=1}^{t} I_{t-s} w_s$. Generation time (GT), which refers to the time interval between the infection of an individual (the primary case) and the subsequent infection of another individual (the secondary case) by the primary case is typically approximated by serial interval (SI) [43]. The function w_s corresponds to the distribution function of SI, where SI can be defined as the time interval between the onset of symptoms in the primary case and the subsequent appearance of symptoms in the secondary case. In the context of fitting the SI distribution, the gamma distribution is commonly selected as the preferred distribution type.

We assume that the occurrence of new cases follows a Poisson distribution, with mean $R_t\Lambda_t$. Therefore, the likelihood of I_t is

$$P(I_t|I_0,\ldots,I_{t-1},w,R_t)=\frac{(R_t\Lambda_t)^{I_t}e^{-R_t\Lambda_t}}{I_t!}, \tag{1}$$

where I_t denotes the daily count of newly reported cases. However, the estimation of R_t using this approach is characterized by high volatility and substantial uncertainty. To address this issue, a time window is defined, where the transmissibility is assumed to be constant within the interval $[t-\tau+1,t]$. Within this specified time frame, the reproduction number is denoted as $R_{t,\tau}$. The likelihood of the incidence during this time period $I_{t-\tau+1},\ldots,I_t$ is

$$P(I_{t-\tau+1},\ldots,I_t|I_0,\ldots,I_{t-\tau},w,R_{t,\tau})=\prod_{s=t-\tau+1}^{t}\frac{(R_{t,\tau}\Lambda_s)^{I_s}e^{-R_{t,\tau}\Lambda_s}}{I_s!}. \tag{2}$$

The prior distribution of $R_{t,\tau}$ is specified as a gamma distribution with parameters (a,b). Within the Bayesian framework, the posterior joint distribution of $R_{t,\tau}$ is derived as

$$\begin{aligned}
&P(I_{t-\tau+1},\ldots,I_t,R_{t,\tau}|I_0,\ldots,I_{t-\tau},w)\\
&=P(I_{t-\tau+1},\ldots,I_t|I_0,\ldots,I_{t-\tau},w,R_{t,\tau})P(R_{t,\tau})\\
&=\Big(\prod_{s=t-\tau+1}^{t}\frac{(R_{t,\tau}\Lambda_s)^{I_s}e^{-R_{t,\tau}\Lambda_s}}{I_s!}\Big)\Big(\frac{R_{t,\tau}^{a-1}e^{-\frac{R_{t,\tau}}{b}}}{\Gamma(a)b^a}\Big)\\
&\propto R_{t,\tau}^{a+\sum_{s=t-\tau+1}^{t}I_s-1}e^{-R_{t,\tau}\left(\sum_{s=t-\tau+1}^{t}\Lambda_s+\frac{1}{b}\right)}\prod_{s=t-\tau+1}^{t}\frac{\Lambda_s{}^{I_s}}{I_s!}
\end{aligned} \tag{3}$$

Therefore, the posterior distribution of $R_{t,\tau}$ is a gamma distribution with parameters $\left(a+\sum_{s=t-\tau+1}^{t}I_s,\frac{1}{\frac{1}{b}+\sum_{s=t-\tau+1}^{t}\Lambda_s}\right)$. In our computational analysis, we implemented the serial interval distributions for various variants, including Beta, Alpha, Omicron, and the influenza virus. The serial interval of each virus is assumed to follow a gamma distribution, with a mean of 4 days and a standard deviation of 3 days for the Beta variant [44], a mean of 4.7 days and a standard deviation of 2.9 days for the Delta variant [45], a mean of 3.5 days and a standard deviation of 2.4 days for the Omicron variant [46], and a mean of 3.6 days and a standard deviation of 1.4 days for influenza [47]. For influenza surveillance data, due to the fluctuations in the number of samples collected weekly, with potentially only single-digit samples in a given week, we perform a 4-week moving average smoothing to address this challenge. (shown in Fig. 1) As shown in Fig. 2, we perform 7-day moving average for COVID-19 data. All statistical computations were performed using the 'EpiEstim' package of R-software version 4.2.1.

2.3 Time series models

In the context of short-term epidemic forecasting, ARIMA models have been extensively applied [48–50]. An ARIMA model consists of three main components: the autoregressive

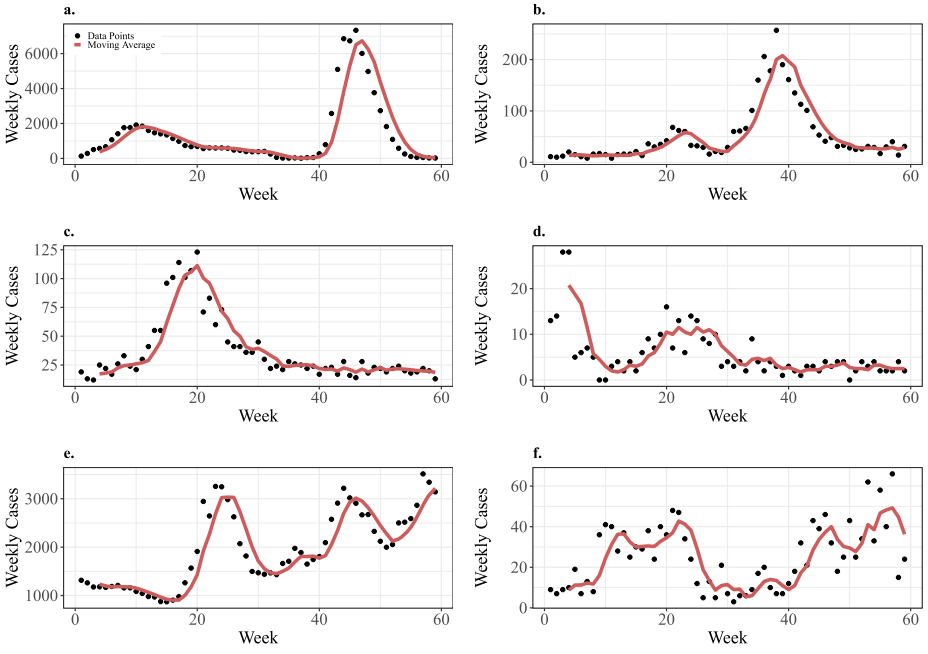

Figure 1 The original data and moving average of influenza across countries. a. China. b. the United Kingdom. c. the United States. d. South Africa. e. Singapore. f. Indonesia

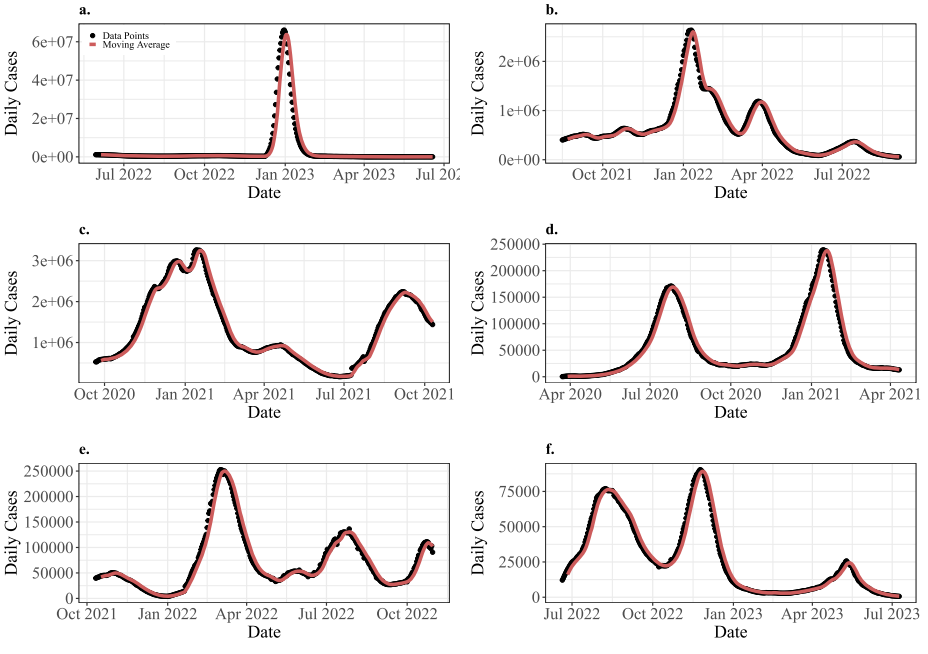

Figure 2 The original data and moving average of COVID-19 across countries. a. China. b. the United Kingdom. c. the United States. d. South Africa. e. Singapore. f. Indonesia

(AR) part, the integrated (I) part, and the moving average (MA) part. Given the seasonal nature of influenza, we employ a seasonal ARIMA (SARIMA[p,d,q][P,D,Q]s) model for the forecasting task. In a SARIMA(p,d,q)(P,D,Q)s model, the parameters p, d, and q represent

the order of the AR, the degree of differencing, and the order of the MA, respectively. The parameters P, D, Q, and s denote the order of the seasonal AR, the order of seasonal differencing, the order of the seasonal MA, and the length of the seasonal cycle, respectively. The steps involved in applying a SARIMA$(p,d,q)(P,D,Q)s$ approach are as follows:

a) *Identification*: an approach to identify which type of ARIMA model is appropriate for the data is addressed. We need to consider whether the time series is stationary by using the augmented Dickey–Fuller test. If the time series is non-stationary, 1-time difference and 1-time seasonal difference should be applied. When stationarity has been achieved, we can examine the patterns in the autocorrelation function (ACF) and partial ACF (PACF) plots to specify the appropriate ARIMA model structure, including the order of the AR and MA components, as well as any necessary seasonal terms.

b) *Parameter selection*: d and D are based on differencing, while initial guesses for p, q, P, and Q can be determined based on patterns in the ACF and PACF plots. Subsequently, other values can be tested and monitored with Akaike's Information Criterion (AIC). Models with the smallest AIC are usually the best. Additionally, the Ljung-Box test is used to conclude whether the series is white noise. With a P-value of <0.05, the hypotheses of independence are all rejected.

c) *Forecasting*: we use seasonal ARIMA models and the three-year pre-pandemic data from each country to estimate the weekly influenza positivity rates in a counterfactual scenario without the COVID-19 outbreak and associated containment measures, covering the period from the onset of the pandemic until six months after reopening. Additionally, we use seasonal ARIMA models and the data from each country during the COVID-19 period to estimate the weekly influenza positivity rates in a counterfactual scenario with the continued presence of the COVID-19 pandemic, also covering the six months after reopening. Descriptive statistics, time-series analyzes and figure plotting were conducted using R-software version 4.2.1.

3 Results

3.1 Transmissibility of COVID-19 before and after lifting of restrictions

The effective reproduction number (R_t) of COVID-19 in China, the United States, and Singapore was reported by using maximum likelihood estimation and Bayesian posterior inference based on daily incidence data, covering a period of 6 months before and 6 months after the lifting of restrictions in each country. In China, the nationwide lifting occurred on December 8, 2022, as shown in Fig. 3a, while the United States relaxed lockdown measures on April 2, 2020, with the corresponding R_t values depicted in Fig. 3b. In Singapore, restrictions were lifted on April 26, 2022, with R_t values shown in Fig. 3c for the same six-month periods.

Following the discovery of the first case of COVID-19 in China on December 31, 2019, the Chinese government implemented rigorous control measures. These measures were adjusted based on the severity of the epidemic in different provinces. For instance, in the case of the severe outbreak in Wuhan at the beginning of 2020, the first-level (highest) emergency response, i.e., a city-wide lockdown policy, was implemented. As a result of these stringent measures, the transmission of COVID-19 in China remained effectively controlled until the complete lifting of restrictions. R_t remained in the vicinity of 1, fluctuating within a narrow range.

The government announced the lifting of restrictions on December 8, 2022 (t = 193). In contrast to other countries, China maintained stringent control measures throughout

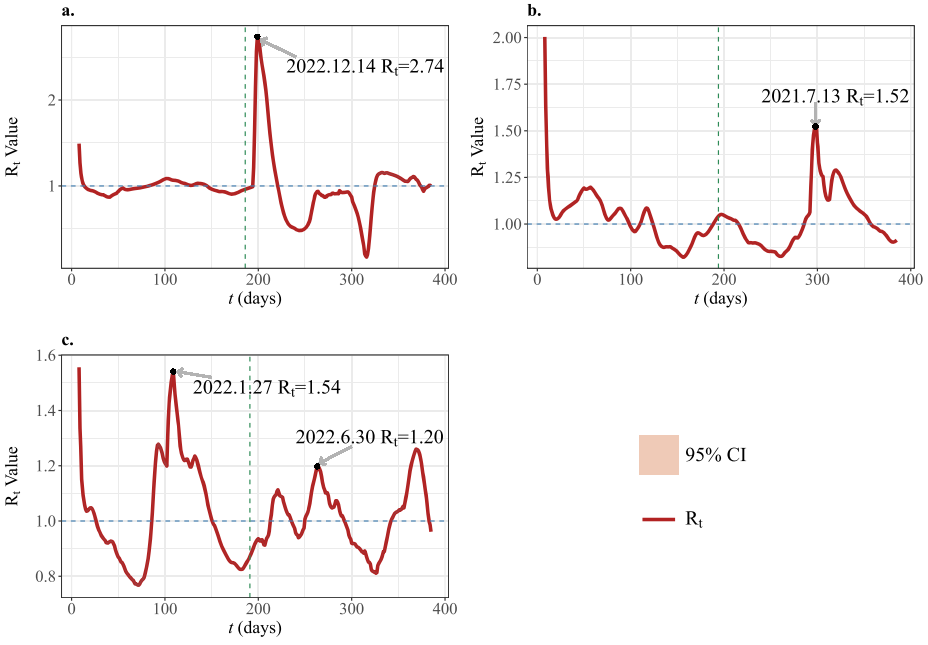

Figure 3 The effective reproduction number data of COVID-19 in a period of 6 months before and 6 months after the lifting of restrictions. a. China. b. the United States. c. Singapore. The horizontal blue dashed line represents the threshold value $R_t = 1$. The vertical green dashed line indicates the designated time frame for lifting restrictions. The red-shaded area represents the 95% confidence interval

the two-year period of the COVID-19 pandemic, resulting in a significant reduction in inter-provincial population mobility. Despite a high national vaccination rate of 91.6%, the densely populated nature of the country, coupled with the majority of individuals being susceptible due to first-time infections and the weakened immune response against the virus, led to a rapid increase in COVID-19 transmission following the lifting of restrictions. The value of R_t reached its peak at 2.74 on December 14, 2022 (t = 199), and subsequently declined rapidly to below 1 after January 5, 2023 (t = 221).

Several factors contributed to this situation. Firstly, the virus had undergone several mutations, resulting in reduced virulence and a significant decrease in fatality rates compared to earlier stages of the pandemic. Therefore, many infected individuals chose to self-isolate at home rather than seek medical treatment in hospitals. Secondly, daily mandatory nucleic acid amplification testing (NAAT) was discontinued at this stage, making it more challenging to quantify the number of asymptomatic infections. These factors collectively contributed to the potential underestimation of the true extent of COVID-19 transmission.

In the case of the US, it is evident that R_t exhibits a gradual reduction on the left side of the gray dashed line. This decline persisted until February 23, 2021 (t = 156), when it reached its minimum value of 0.82. Subsequently, R_t fluctuated around 0.9, indicating successful control of the number of cases and deaths. Following the complete relaxation of restrictions, within the initial 100 days, R_t fluctuated around 1. However, on July 13, 2021 (t = 298), it rose to 1.52. This increase can be attributed to the policy proposed by the United States government on July 9, 2021, advocating for the resumption of in-person instruction [51]. Besides, the emergence of the Delta variant in the United States dur-

ing July 2021 was a significant development in the pandemic. This novel viral strain possessed heightened transmissibility characteristics as well as an increased ability to evade immune responses. As a result, the appearance of the Delta variant triggered a fresh wave of elevated infection rates, leading to a renewed infection peak across the country. Subsequently, on July 28, 2021, the CDC issued recommendations on masking in public indoor settings to mitigate the spread of the Delta variant [52]. Consequently, R_t gradually declined below 1, indicative of the situation being brought under control.

For Singapore, it can be observed that the values of R_t initially remained below 1, disregarding the periods when R_t exceeded 1 due to the inaccuracy of the starting and ending segments. However, towards the end of 2021, with the incursion of the Omicron variant [53], despite the implementation of stringent containment measures by the Singaporean government, transmission continued to escalate. It reached its peak on January 27, 2022 (t = 109) with an R_t value of 1.54. Subsequently, relying on NPIs and robust healthcare support from the government, R_t gradually declined to levels below 1. On April 26, 2022, the Singaporean government made the decision to lift restrictions comprehensively. Following the lifting of restrictions, R_t exhibited a gradual increase, reaching 1.11 on May 19, 2022 (t = 221), before being brought under control and decreasing below 1. On June 21, 2022 (t = 254), there was a rise in BA.4 and BA.5 subvariant cases [54], resulting in a rapid rise in R_t. It reached a localized peak of 1.20 on June 30, 2022 (t = 263), after which R_t fluctuated around 1. On October 14, 2022 (t = 369), R_t reached its peak value of 1.26 since the lifting of restrictions. The Singapore Ministry of Health announced the tightening of safe management measures for in-person visits to hospitals and residential care homes from October 14, 2022, to November 10, 2022, aligning with the intensified spread of the disease during that period [55].

Overall, R_t trends reflect the complex interplay of control measures, viral mutations, and public health responses across these countries, illustrating how reopening policies influenced COVID-19 dynamics. Correspondingly, the impact of the lifting of restrictions on influenza is detailed in the Supporting Information Appendix A.

3.2 Comparative analysis of COVID-19 and influenza transmission dynamics in the context of lifting pandemic restrictions

The countries were categorized into three groups based on whether the timing of lifting COVID-19 restrictions coincided with the seasonal influenza period. Countries where the lifting of restrictions occurred around the influenza season, represented by China and the United Kingdom; countries where the lifting took place outside the typical influenza season, represented by the United States and South Africa; and countries situated in the tropics without a well-defined influenza season, represented by Singapore and Indonesia. This section first conducts a comparative assessment of the effective reproduction number (R_t) of COVID-19 across the three country groups during the 6-month periods before and the 6-month periods after lifting pandemic restrictions. It then performs a comparative evaluation of influenza R_t dynamics within the same time frame and country groupings. Finally, the characteristics of COVID-19 and influenza transmission trends within each group after lifting restrictions, as well as the impact of the post-restriction COVID-19 dynamics on influenza transmission are examined in detail.

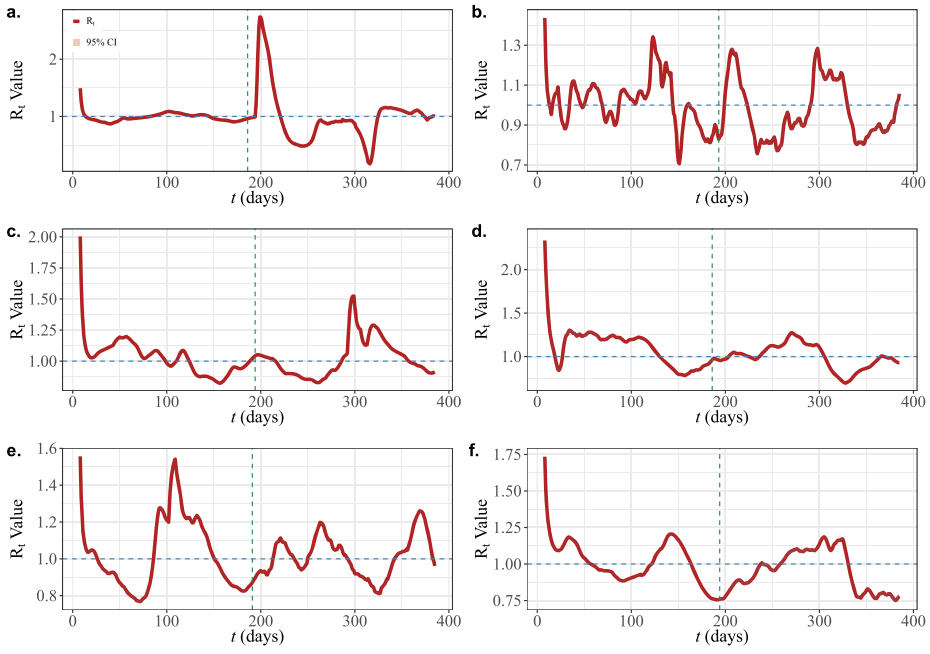

Figure 4 The effective reproduction number of COVID-19 across countries. a. China. b. the United Kingdom. c. the United States. d. South Africa. e. Singapore. f. Indonesia. The horizontal blue dashed line represents the threshold value $R_t = 1$. The vertical green dashed line indicates the designated time frame for lifting restrictions in different countries. The red-shaded area represents the 95% confidence interval

3.2.1 Comparison of the transmissibility of COVID-19 across countries

Due to significant differences in climate, policy frameworks, economic development and medical levels across countries, the transmission rates of COVID-19 before and after reopening have varied considerably between nations. The COVID-19 control policies of China have become highly refined after two years of implementation, and even with the introduction of new variants, the effective reproduction number (R_t) has remained below 1.1. After lifting restrictions, the R_t quickly rose to 2.74, leading to rapid nationwide spread, but then rapidly decreased to below 1, as shown in Fig. 4a. The United Kingdom government's strategy was to manage COVID-19 and achieve herd immunity through infection. After experiencing three waves of the pandemic, the UK lifted the lockdown and other preventive measures on February 24, 2022 (t = 193). As shown in Fig. 4b, the R_t began a precipitous ascent commencing December 13, 2021 (t = 120), peaking at 1.34 on December 16, 2021 (t = 123), before subsiding below 1 on January 7, 2022 (t = 145). This fluctuation was attributed to the incursion of the Omicron variant from South Africa in December 2021, which caused a record-breaking surge in cases. The post-reopening era in the UK witnessed a substantial amplification of COVID-19 transmission, as evinced by the R_t exceeding 1 on March 2, 2022 (t = 199) and culminating in a peak of 1.28 on March 10, 2022 (t = 207) before receding below 1 on March 27, 2022 (t = 224). However, the R_t rose above 1 again starting June 2, 2022 (t = 291), peaking at 1.28 on June 9, 2022 (t = 298), before declining to below 1 on July 11, 2022 (t = 330). This resurgence was attributed to the emergence of the new Omicron subvariants BA.4 and BA.5 in June 2022, which exhibited heightened transmissibility and immune evasion capabilities. Although the UK government implemented supplementary social distancing measures to curtail dissemi-

nation, the effects were limited until BA.4 and BA.5 became the dominant strains and the outbreak was eventually brought under control.

As depicted in Fig. 4c, the epidemiological trajectory in the United States exhibited gradual subsidence of the pandemic prior to reopening measures. The post-reopening period witnessed a modest resurgence in transmission, which was swiftly contained. However, the subsequent incursion of the Delta variant, coupled with the resumption of in-person instruction, facilitated a widespread dissemination of COVID-19 across the nation. On March 15, 2020, the President of South Africa declared a state of national calamity, initiating a series of containment measures, such as suspending educational institutions and enforcing limited restrictions on selected sea and land entry points to combat the COVID-19 pandemic. South Africa experienced its first peak of COVID-19 cases from June to mid-July 2020 ($t = 71 - 115$), as depicted in Fig. 4d, with R_t fluctuating around 1.20. Subsequently, the situation gradually came under control, and the spreading decreased. The South African government announced the lifting of restrictions on October 1, 2020 ($t = 193$). However, due to the dominant emergence of the 501Y.V2 variant, the country entered its second wave of the pandemic, as declared by the South African Department of Health in December 2020. R_t reached its peak at 1.27 on December 8, 2020 ($t = 271$), and began to decline below 1 from January 22, 2021 ($t = 306$), fluctuating around 0.8, which indicates that the second wave of the pandemic was subsequently brought under control.

As depicted in Fig. 4e, the incursion of the Omicron variant precipitated a substantial surge in COVID-19 transmission within Singapore, even as the government implemented stringent lockdown and restriction policies. Despite these measures, the spread continued to escalate. However, following the lifting of restrictions, while COVID-19 transmission did expand to a certain degree, it was quickly brought under control. Subsequent to this, the invasion of the BA.4 and BA.5 variants triggered a renewed wave of COVID-19 intensification in Singapore. Figure 4f illustrates the changes in the Rt values for Indonesia during the six months preceding and following the reopening. Commencing in late October 2022, the infiltration of the BA.4 and BA.5 variants precipitated widespread COVID-19 transmission within Indonesia, with the R_t value peaking at 1.21 on November 8, 2022 ($t = 142$). This was followed by a gradual decline, dropping below 1 after November 30, 2022 ($t = 164$). The Indonesian government announced the reopening on December 30, 2022 ($t = 194$), after which the R_t values exhibited a slow but steady increase, surpassing 1 on March 5, 2023 ($t = 259$). It subsequently fluctuated around 1.2 until it fell back below 1 after May 16, 2023 ($t = 331$), signalling the effective control of the pandemic spread.

As evident in Fig. 4, all the countries displayed an increase in COVID-19 transmission during the six months following the relaxation of public health measures, in contrast to the preceding six-month period. This phenomenon was likely driven by the relaxation of pandemic prevention and control measures, which increased mobility and social interactions among the populace, thereby providing greater opportunities for virus transmission and exposure. Moreover, the prolonged implementation of restrictive policies and NPIs has led to a decline in population-level immunity. When the intensity of control measures was diminished, the proportion of susceptible individuals increased, enabling the virus to spread more rapidly. The trends observed in the US and South Africa exhibited certain similarities, wherein the epidemic was gradually brought under control prior to the reopening, followed by a limited resurgence of transmission after the easing of restrictions, which was then quickly contained. In contrast, the epidemiological dynamics of

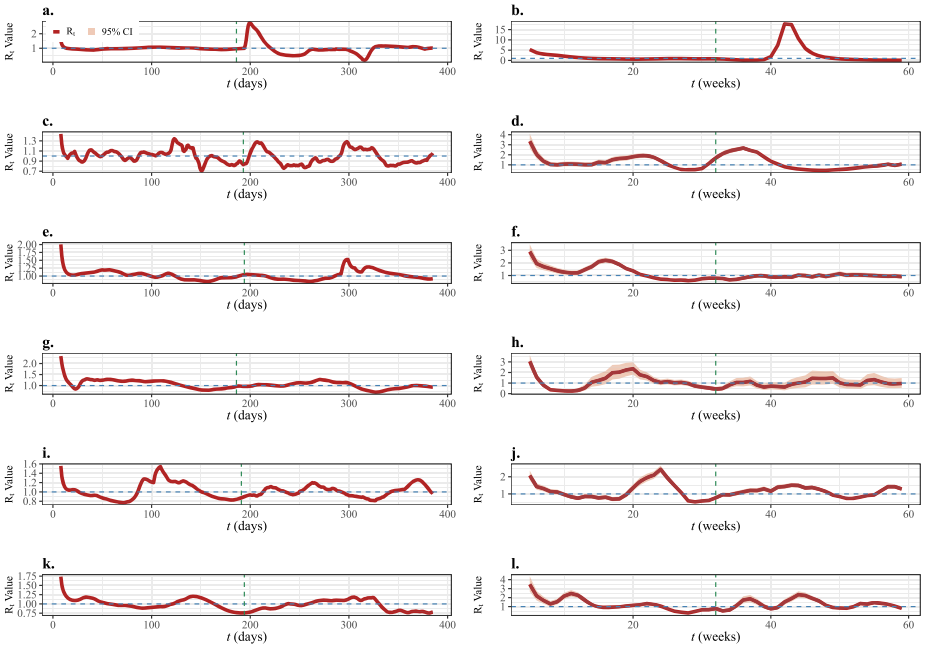

Figure 5 The effective reproduction number of COVID-19 and influenza across countries. a. R_t of COVID-19 in China. b. R_t of influenza in China. c. R_t of COVID-19 in the United Kingdom. d. R_t of influenza in the United Kingdom. e. R_t of COVID-19 in the United States. f. R_t of influenza in the United States. g. R_t of COVID-19 in South Africa. h. R_t of influenza in South Africa. i. R_t of COVID-19 in Singapore. j. R_t of influenza in Singapore. k. R_t of COVID-19 in Indonesia. l. R_t of influenza in Indonesia. The horizontal blue dashed line represents the threshold value $R_t = 1$. The vertical green dashed line indicates the designated time frame for lifting restrictions. The red-shaded area represents the 95% confidence interval

Singapore and Indonesia were somewhat analogous, characterized by a surge in COVID-19 spread driven by the incursion of new variants prior to the reopening phase, which was subsequently brought under control. However, the post-reopening period witnessed a more pronounced increase in virus transmission in these countries, though the regional peak values were slightly higher in the US and Singapore. The divergence in R_t profiles between the UK, China, and the other nations is likely attributable to variations in national pandemic control policies and climatic factors. Correspondingly, the comparison of the transmissibility of influenza after reopening is detailed in the Supporting Information Appendix B.

3.2.2 Comparative analysis of COVID-19 and influenza transmission patterns

Figure 5 presents a comparative analysis of the R_t trends for COVID-19 and influenza in China, the UK, the US, South Africa, Singapore, and Indonesia, covering the 6-month periods before and after their respective lifting of restrictions.

The comparative analysis of the trends in COVID-19 and influenza across the six countries reveals several notable patterns. Broadly speaking, the trajectories of expansion and decline for the two respiratory illnesses within the same country tend to exhibit similar overall trends. But there are distinct temporal differences, with COVID-19 typically leading the transmission dynamics. Specifically, the results indicate that COVID-19 transmission tends to peak and begin declining before influenza comes to the forefront. In many instances, as the R_t values of COVID-19 start decreasing, the R_t values of influenza then

begin to increase. Rare are the occurrences where both the R_t values of COVID-19 and influenza are simultaneously greater than 1. More commonly observed are the scenarios where the R_t values of COVID-19 are greater than 1 while the R_t values of influenza remain below 1, or vice versa, suggesting that at a given time, the majority of the population is affected by only one of the two respiratory pathogens. This pattern suggests a general lack of substantial concurrent widespread transmission of COVID-19 and influenza within the same populations.

This comprehensive set of graphs allows for a direct comparison of the transmission dynamics of COVID-19 and influenza in these six countries, both before and after their reopening events, thereby indicating that the two respiratory illnesses cannot typically exhibit large-scale co-circulation at identical time points.

3.3 Impact of COVID-19 lifting of restrictions on influenza incidence trends

The weekly influenza positivity rate data was utilised in this section, which was from the three years preceding the onset of the COVID-19 pandemic, as well as the weekly influenza positivity data during the COVID-19 period, as the training dataset. A seasonal ARIMA modeling approach was applied to independently forecast the post-reopening influenza positivity rates for each country. The detailed justification for the parameter selection is shown in the Supporting Information Appendix C. By comparing the forecasted influenza positivity rates in the counterfactual scenario without the COVID-19 pandemic to the actual post-reopening influenza positivity rates, as well as the forecasted influenza positivity rates assuming the continued presence of the COVID-19 pandemic to the actual post-reopening influenza positivity rates, two types of counterfactual experiments are conducted. This allows for the observation of the impact of COVID-19 reopening policies on influenza transmission dynamics.

As shown in Fig. 6a, the red line shows actual influenza positivity rates before and during the pandemic in China. The blue dashed line represents forecasted rates in a hypothetical no-COVID-19 scenario, revealing typical seasonal peaks prior to the outbreak. The national lockdown led to a rapid decline in influenza positivity to nearly 0% in early 2020. In late 2021, as China maintained its dynamic zero-COVID strategy, the lockdown measures were partially eased, allowing for some restoration of population mobility. Therefore, the positivity rate gradually returned to a normal trend, peaking at 31.5%, significantly lower than the 40%+ peaks seen in previous years. A further atypical peak occurred in mid-2022, likely due to the lockdown's disruption of typical transmission dynamics, resulting in a build-up of susceptible individuals who had not been exposed to influenza viruses for an extended period.

The orange line indicates actual influenza rates over the six months following the lifting of restrictions. After the lifting of restrictions, the positivity rate surged to 53.2%, exceeding the 42.8% peak predicted for a no-pandemic scenario, and occurred about 10 weeks later than expected.

During the stringent lockdown policies in 2020, the influenza positivity rate remained near 0, rendering the inclusion of that data segment in the time series forecasting of limited research values. The green dashed line in Fig. 6a represents the influenza trend forecast based on the empirical data from the period of policy relaxation. The model forecasted a seasonal influenza peak in late 2022 and early 2023 at around 25% in the absence of reopening, while actual conditions resulted in a delayed but more severe peak of 53.2%, doubling

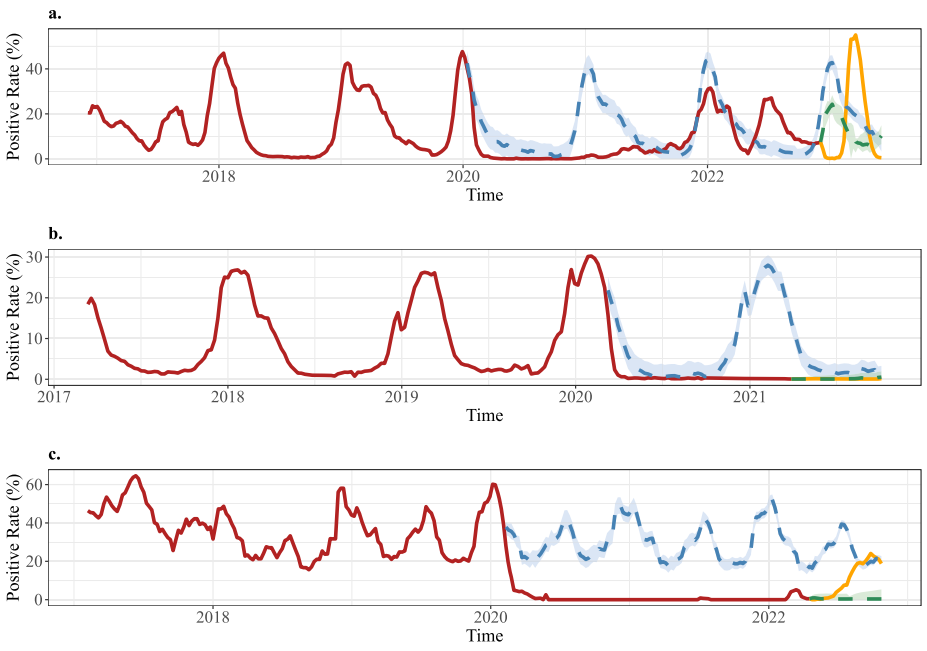

Figure 6 Observed and predicted influenza test positivity rate from 2017 to 2023. a. China. b. the United States. c. Singapore. The red line represents the actual historical influenza positivity rates prior to the reopening period. The orange line depicts the actual influenza positivity rates observed during the post-reopening period. The blue dashed line shows the time series forecasts of influenza positivity rates during the pandemic period and the post-reopening phase, based on the preceding three years of data. The blue-shaded region indicates the 95% confidence interval around these forecasts. The green dashed line illustrates the time series forecasts of influenza positivity rates assuming the continued presence of the ongoing COVID-19 pandemic, using the actual pandemic-era data as the input. The yellow-shaded region represents the 95% confidence interval for these forecasts

the anticipated figure. Conversely, the implementation of reopening policies has led to a delayed yet more severe influenza peak. The seasonal epidemic apex has shifted by several weeks, and the observed peak positivity rate has doubled to around 53.2%, significantly exceeding the 25% peak that would have been expected without the pandemic-induced disruptions to disease dynamics.

In the US (shown in Fig. 6b), the red line shows actual influenza positivity rates during the pandemic, which quickly declined to below 1% due to NPIs and lockdown measures. The blue dashed line reflects predicted rates in a no-pandemic scenario. The actual rates declined more rapidly than predicted under NPIs and reached a lower absolute value. The orange line represents the actual influenza positivity rate data for the 6-month period following the lifting of restrictions. The actual influenza positivity rate data is noticeably lower than the predicted data, remaining around 0.1% after reopening, coinciding with the end of the typical influenza season, resulting in minimal fluctuations. The green dashed line illustrates the influenza positivity rate forecast based on the data from the period of policy relaxation, aligning closely with observed rates.

As illustrated in Fig. 6c, the red line depicts actual influenza positivity rates before and during the pandemic in Singapore. Following intervention measures in early 2020, influenza positivity rates dropped to 0 and remained low, with a minor peak of 5.2% in early 2022, attributable to limited sampling. The blue dashed line shows predicted influenza positivity rates in a no-COVID scenario, highlighting a quicker decline to 0 during lock-

downs. The orange line shows post-reopening influenza positivity rates, which gradually normalized, peaking at 24.1%, lower than the 20%-60% range seen before the pandemic. The predicted wave-like pattern in the absence of pandemic impacts did not materialize, as actual rates exceeded predictions shortly after reopening, suggesting a gradual recovery of influenza activity.

The green dashed line represents the influenza positivity rate forecast based on the data from the period of policy relaxation. The stringent lockdowns effectively controlled influenza transmission, maintaining rates near 0. However, the influenza positivity rate rose immediately after the lifting of restrictions, which proved that the lockdown policies utilized by Singapore have a strong depressive effect on influenza.

4 Discussion

In this research, we classified countries into three categories based on whether the timing of their lifting of restrictions coincides with the seasonal fluctuations of influenza: those reopening near the influenza season, those reopening outside the influenza season, and those in the tropics without a defined influenza season. The effective reproduction number (R_t) for COVID-19 and influenza was calculated in the six months before and after reopening for each country category in this study, linking the epidemiological trends to the policy changes. The results showed that COVID-19 transmission increased after reopening in all countries, potentially due to the introduction of new variants, but remained manageable overall. This study found that the dynamics of influenza transmission underwent significant changes after the lifting of restrictions, with varying effects observed across different countries. For the first country group, reopening delayed the peak of influenza transmission. For the second group, reopening shortened the seasonal fluctuation of influenza compared to pre-pandemic patterns. For the third group, reopening led to an increase in influenza transmission. While the general trends were similar within each country group, the specific transmission dynamics varied due to differences in policies and climates, with COVID-19 typically preceding influenza activities. Furthermore, we used time series models to project influenza positivity rates for the three country groups under scenarios with and without the ongoing pandemic. In China, the influenza activity season shifted from a single annual peak to two peaks during the lockdown period, with the peak positivity rate decreasing from 43.1% to 31.5%. After the lifting of restrictions, the influenza peak was delayed by 10 weeks compared to both the pre-pandemic scenario and the continued pandemic scenario, and the overall influenza activity increased from 42.8% to 55.1%. In the United States, the influenza season remained in the off-season for the first six months after reopening, with the observed values lower than the predicted seasonal pattern but still below 1%. In Singapore, influenza activity gradually increased from 0 to 24.1% after reopening, similar to the predicted maximum of 21.5% in the absence of the pandemic. Compared to previous research, our study clearly elucidates the direct impact of lifting restrictions on influenza transmission, particularly in countries that reopened near the influenza season.

A substantial strength of our research also lies in the incorporation of the timing of the lifting of the epidemic in each country. Prior studies have made comparisons between COVID-19 and influenza transmission, as well as the impact of NPIs after COVID-19 on influenza spread. However, these studies were often conducted during the outbreak or ongoing phases of the pandemic, leaving the effects of reopening on the transmissibility of

COVID-19 and influenza unclear. Our research is able to address these gaps, providing new perspectives to prepare for potential outbreaks after reopening. Furthermore, unlike other studies, which selected research countries in a more general manner, this study classified nations based on the proximity of their reopening timeline to the influenza season. This approach allows for broadly applicable conclusions drawn from the findings. Finally, we conducted counterfactual experiments using the lifting of restrictions as the pivot point. Such large-scale, global lockdowns are rare occurrences, and these counterfactual analyzes can provide clear descriptions of how influenza transmission dynamics changed under the influence of the COVID-19 pandemic and control measures. Collectively, these strengths of the study design and analytical approach distinguish this research and enhance its value in informing public health preparedness and policies in the post-pandemic era.

Regarding the limitations of this research, first, the observed positivity rates may be affected by biases in virological surveillance, such as sample collection rates and case selection. For example, in countries with small sampling volumes like Singapore, the influenza positivity rate was essentially 0 during the COVID-19 pandemic, indicating potential underestimation of the data used in this study. Improved data quality could enhance the accuracy of the research findings. Secondly, while the ARIMA model is a well-established forecasting method, it cannot fully account for factors such as virus strain types, the severity of control measures, and individual behavioral patterns that influence infectious disease transmission dynamics. Moreover, the ARIMA model is more suitable for short-term predictions, with relatively poorer performance for long-term forecasts. Analyzing long-term data could provide deeper insights into the lasting impacts of the COVID-19 pandemic and its mitigation measures on influenza transmission.

5 Conclusion

In conclusion, our research has improved the understanding of how the lifting of COVID-19 interventions impacts influenza transmission. After reopening, with waning immunity to influenza, the upcoming influenza season is likely to face a high risk of major outbreaks. Therefore, assessing the influence of COVID-19 reopening on influenza virus transmission is crucial, and proactive planning for healthcare management and public health policies should be able to mitigate this risk. The findings from this study provide insights into the complex interplay between COVID-19 control measures and influenza epidemiology. As societies navigate the post-pandemic landscape, this analysis highlights the importance of considering the potential downstream effects on other respiratory pathogens when making decisions about COVID-19 restrictions. Careful monitoring and forward-looking policies are essential to protect public health and manage the dual burden of these co-circulating infectious diseases in the future.

Appendix A: Transmissibility of influenza before and after lifting of restrictions

The R_t of influenza for China is illustrated in Fig. 7, where the red line represents the 55-week R_t, the light red shaded area represents the 95% confidence interval, the blue dashed line denotes an R_t value of 1, and the green dashed line indicates the lifting of COVID-19 restrictions in Singapore.

Influenza in China exhibits a pronounced seasonal pattern, with winter and spring constituting the peak seasons for its prevalence. Typically, the peak interval spans from the

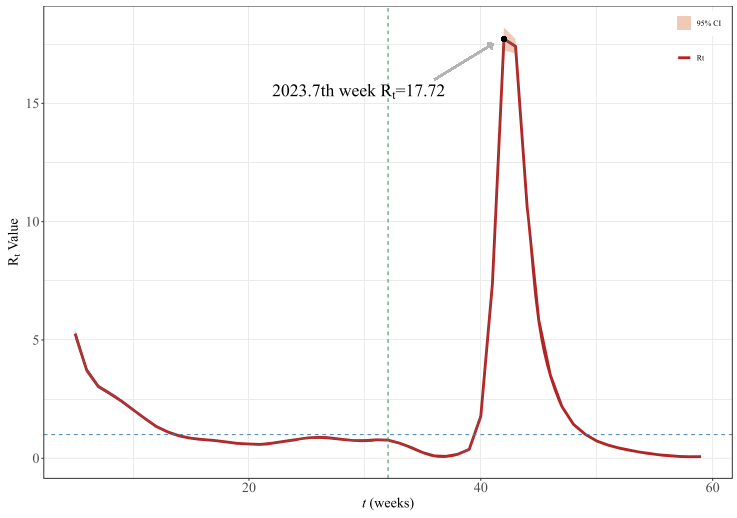

Figure 7 The effective reproduction number data of influenza in a period of 6 months before and 6 months after the lifting of restrictions in China. The horizontal blue dashed line represents the threshold value $R_t = 1$. The vertical green dashed line indicates the designated time frame for lifting restrictions. The red-shaded area represents the 95% confidence interval

49th week of the previous year to the 6th week of the following year. As illustrated in Fig. 7, the R_t values remained consistently below 1 until week 5 of 2023 ($t = 40$). Starting from the 5th week, R_t rapidly escalated and reached its peak of 17.72 in the 7th week of 2023 ($t = 42$). Subsequently, it underwent a swift decline, falling below 1 after week 15 of 2023 ($t = 50$), indicating effective control of influenza transmission. Notably, according to conventional patterns, the seasonal influenza peak in China should have transpired between $t = 32$ and $t = 41$. Nevertheless, stringent government measures pertaining to outbreak prevention and containment resulted in a two-month delay in the onset of the influenza epidemic.

During the early stages of relaxation measures, the general public exhibited a high level of awareness and compliance, characterized by voluntary adherence to practices such as mask usage, maintenance of social distancing, and avoidance of densely populated public venues. The 5th week of 2023 marked the conclusion of the Chinese New Year holiday and the beginning of the commencement of the first week of post-holiday work resumption. By this juncture, a two-month period had elapsed since the relaxation of restrictions, and the majority of individuals had resumed their pre-pandemic lifestyles, leading to a significant increase in influenza transmission in the absence of NPIs. Furthermore, the gradual reopening of educational institutions, commencing from the 8th week, engendered the congregation of students within classrooms and campuses, thereby augmenting the opportunities for influenza virus transmission. Consequently, this phase witnessed a sustained exacerbation of influenza transmission dynamics.

By observing historical data, it is evident that the United States experiences an annual peak in influenza outbreaks during the winter and spring seasons, typically occurring between week 48 of the previous year and week 7 of the next year, corresponding to weeks 13 to 23, as depicted in Fig. 8. As shown in Fig. 8, the R_t values began to rise from week 47 of 2020 ($t = 13$), reaching a peak of 2.20 in week 50 of 2020 ($t = 16$). Subsequently, it gradually declined and fell below 1 after the 3rd week of 2021 ($t = 22$). This period aligns with the

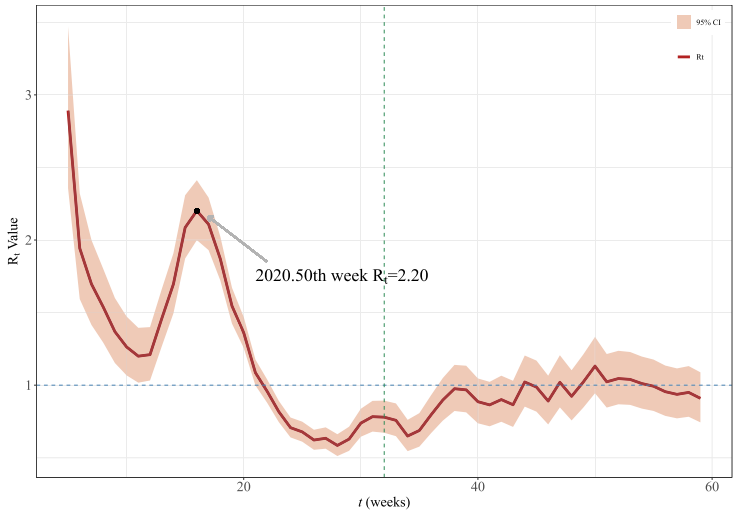

Figure 8 The effective reproduction number data of influenza in a period of 6 months before and 6 months after the lifting of restrictions in the United States. The horizontal blue dashed line represents the threshold value $R_t = 1$. The vertical green dashed line indicates the designated time frame for lifting restrictions. The red-shaded area represents the 95% confidence interval

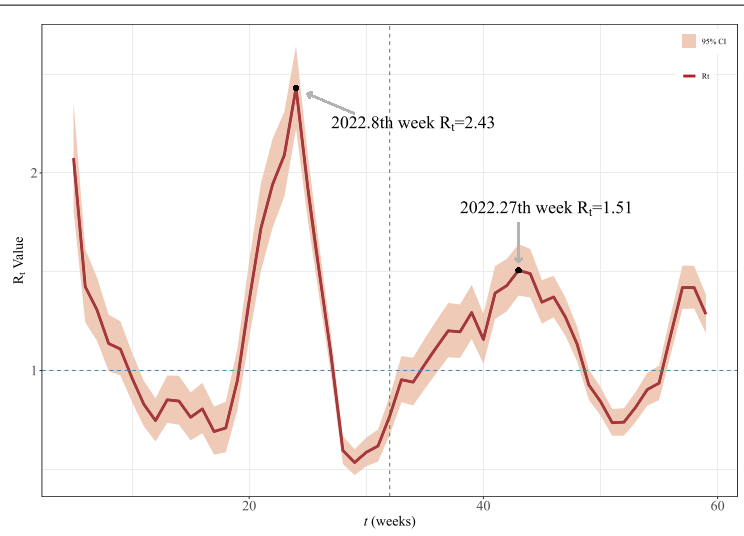

Figure 9 The effective reproduction number data of influenza in a period of 6 months before and 6 months after the lifting of restrictions in Singapore. The horizontal blue dashed line represents the threshold value $R_t = 1$. The vertical green dashed line indicates the designated time frame for lifting restrictions. The red-shaded area represents the 95% confidence interval

seasonal peak of influenza in the US. Although restrictions were not entirely lifted during this time, influenza transmission did not cease. Following the easing of restrictions, the R_t values remained around 1, fluctuating with a maximum value not exceeding 1.13. This indicates a low-level transmission of influenza during non-peak seasons.

The R_t of influenza for Singapore is shown in Fig. 9, where the black line represents the 55-week R_t, the light blue shaded area represents the 95% confidence interval, the

red dashed line denotes an R_t value of 1, and the gray dashed line indicates the lifting of COVID-19 restrictions in Singapore.

In contrast to countries with pronounced seasonal variations, Singapore exhibits a relatively stable climate devoid of distinct seasonal patterns. As a result, influenza maintains a year-round presence in Singapore rather than being confined to specific seasons. As depicted in Fig. 9, the R_t values exhibited an upward trend commencing in week 4 of 2022 ($t = 20$), reaching a peak of 2.43 in week 8 ($t = 24$) before declining. Within three weeks, it fell below 1, indicative of effective control of influenza transmission. The 4th week of 2022 coincided with the Lunar New Year and the Spring Festival, leading to increased social gatherings, events, and travel, which facilitated the spread of the influenza virus. Additionally, the Ministry of Education in Singapore announced that the Term I of Semester I of the academic calendar for schools spanned from January 4, 2022, to March 11, 2022, covering weeks 1 to 10. The resumption of student activities after the commencement of the academic year contributed to the intensified propagation of influenza.

Following the easing of restrictions, the R_t values remained below 1 for the subsequent 6 weeks, surpassing this threshold after week 19 of 2022 ($t = 35$) and exhibiting a gradual upward trajectory. Eventually, R_t reached its zenith of 1.51 in week 27 ($t = 43$) before gradually declining and falling below 1 after the 32nd week of 2022 ($t = 48$). The observed temporal dynamics can be attributed to multiple factors. Firstly, this period coincided with Singapore's tropical rainy season, characterized by hot and humid climatic conditions that favor the survival and transmission of the influenza virus. Moreover, such environmental conditions tend to compromise the host's immune response, rendering individuals more susceptible to infection. Secondly, the Ministry of Education issued a directive designating the period from May 27, 2022, to June 26, 2022, as the summer vacation, during which students ceased congregating in schools, resulting in reduced interpersonal contacts and subsequently attenuated influenza transmission. However, the frequency of activities such as summer camps, travels, and gatherings increased significantly during the vacation period, leading to an elevated risk of influenza transmission. As a result, the R_t values remained around 1.26 from the 22nd ($t = 38$) to the 25th week ($t = 41$). Following the resumption of the Semester II on June 27, 2022, R_t exhibited a rapid surge, which was subsequently brought under control in August.

Appendix B: Comparison of the transmissibility of influenza across countries

The analysis is based on six countries: China, the United States, Singapore, the United Kingdom, South Africa, and Indonesia. These countries can be classified into three categories based on the criteria mentioned earlier.

The first category encompasses countries where the reopening near the typical influenza seasonal peak, exemplified by China and the UK. The effective reproduction number (R_t) of influenza profiles for these nations during the six-month periods before and after the reopening are illustrated in Fig. 10a and Fig. 10d, respectively.

Both China and the United Kingdom exhibit pronounced seasonality in their influenza dynamics. In the case of China, the nation typically experiences influenza peaks between the 49th week of the first year and the 6th week of the subsequent year. However, after the reopening of China occurred in the 49th week of 2022, the actual influenza peak was observed to be delayed by approximately 8 weeks, manifesting between the 5th and 15th

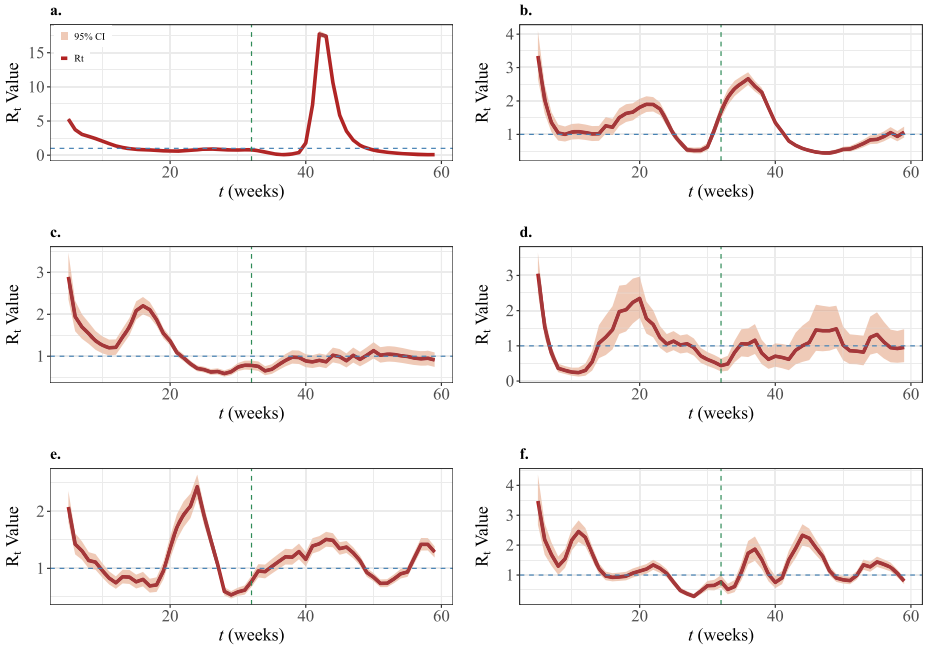

Figure 10 The effective reproduction number of influenza across countries. a. China. b. the United Kingdom. c. the United States. d. South Africa. e. Singapore. f. Indonesia. The horizontal blue dashed line represents the threshold value $R_t = 1$. The vertical green dashed line indicates the designated time frame for lifting restrictions in different countries. The red-shaded area represents the 95% confidence interval

weeks of 2023. This delay can be attributed to the relatively robust implementation of NPIs and self-isolation policies prior to the lifting of restrictions in China. These measures effectively suppressed influenza transmission until the post-reopening period, when increased population mobility and social interactions facilitated the emergence of a new wave of influenza activity.

A similar pattern was observed in the UK, where influenza peaks typically occur between the 45th week of the first year and the 8th week of the following year. However, after the reopening of the UK in the 8th week of 2022, the influenza peak exhibited a bimodal nature, with one peak occurring between the 45th week of 2021 and the 1st week of 2022, and another between the 8th and 16th weeks of 2022. This bimodal pattern can be explained by the fact that, although some mask-wearing and social distancing measures were implemented in the UK, the intensity of these interventions was relatively lower compared to China. Consequently, influenza activity continued to some degree during the nation's typical seasonal peaks, prior to the resurgence of transmission in the post-reopening period. Following the reopening, the influenza seasons in these countries would have been expected to have subsided according to historical patterns. However, the resumption of societal and economic activities led to increased population mobility and interactions, thereby facilitating the emergence of a new wave of influenza transmission.

In summary, the timing of the influenza peaks in China and the UK diverged from their historical seasonal norms following the COVID-19 reopening measures implemented in these countries. The reopening from COVID-19 restrictions had a delaying effect on the timing of the influenza transmission peaks for nations where the reopening occurred in proximity to the typical influenza seasonal dynamics.

The second category includes countries where the timing of the COVID-19 reopening was outside the typical influenza season, such as the United States and South Africa. The R_t values of influenza for these countries during the six months before and after the reopening are shown in Fig. 10b and Fig. 10e, respectively.

The US and South Africa also exhibit strong influenza seasonality. In the US, the influenza seasonal patterns typically occur between the 48th week of the first year and the 8th week of the subsequent year. During the 2020-2021 season, the US influenza peak was observed between the 47th week of 2020 and the 3rd week of 2021. The US government announced the lifting of restrictions in the 13th week of 2021, which was outside the influenza season. After the reopening, the R_t values of influenza in the US fluctuated around 1, indicating a relatively low level of influenza transmission.

South Africa is in the southern hemisphere and typically experiences influenza seasonal peaks between the 20th and 35th weeks of the year. In 2020, the influenza peak in South Africa was observed between the 22nd and 32nd weeks. The South African government announced the reopening in the 40th week of 2020, which was also outside the influenza season. After the lifting of restrictions, the R_t values of influenza in South Africa fluctuated around 1, with a maximum of 1.5, indicating relatively limited influenza transmission.

Therefore, it can be concluded that for countries where the reopening date was near the non-influenza season, the impact of the COVID-19 reopening on influenza transmission was relatively modest, and the seasonal fluctuations in influenza transmission were shorter compared to the pre-pandemic period.

The third category includes tropical countries where influenza does not exhibit a pronounced seasonal pattern. The representative countries examined in this case are Singapore and Indonesia. The R_t values of influenza trends for these two countries during the six months before and after their respective reopenings are shown in Fig. 10c and Fig. 10f.

Despite the fact that the reopening timing in these two countries was separated by approximately half a year, the R_t values of influenza trends are remarkably similar. Both countries experienced a large-scale influenza outbreak prior to their reopenings but were able to quickly bring the transmission under control. Furthermore, the patterns of influenza resurgence after the reopenings were also highly comparable between the two countries. This similarity in the R_t values of influenza dynamics between Singapore and Indonesia is likely attributable to the shared characteristics of tropical climate. The lack of strong influenza seasonality in these tropical nations suggests that the timing of the COVID-19 reopening may have a less pronounced impact on the trajectory of influenza transmission, compared to countries with well-defined influenza seasons.

Appendix C: Justification for the parameter selection in SARIMA

```
models <- list(
    arima(ts_data, order = c(1, 1, 0), seasonal = c(0, 1, 0)),
    arima(ts_data, order = c(1, 1, 0), seasonal = c(1, 1, 0)),
    arima(ts_data, order = c(1, 1, 0), seasonal = c(2, 1, 0)),
    arima(ts_data, order = c(1, 1, 0), seasonal = c(0, 1, 1)),
    arima(ts_data, order = c(1, 1, 0), seasonal = c(1, 1, 1)),
    arima(ts_data, order = c(1, 1, 0), seasonal = c(2, 1, 1)),
    arima(ts_data, order = c(1, 1, 1), seasonal = c(0, 1, 0)),
    arima(ts_data, order = c(1, 1, 1), seasonal = c(1, 1, 0)),
```

```
    arima(ts_data, order = c(1, 1, 1), seasonal = c(2, 1, 0)),
    arima(ts_data, order = c(1, 1, 1), seasonal = c(0, 1, 1)),
    arima(ts_data, order = c(1, 1, 1), seasonal = c(1, 1, 1)),
    arima(ts_data, order = c(1, 1, 1), seasonal = c(2, 1, 1)),
    arima(ts_data, order = c(1, 1, 2), seasonal = c(0, 1, 0)),
    arima(ts_data, order = c(1, 1, 2), seasonal = c(1, 1, 0)),
    arima(ts_data, order = c(1, 1, 2), seasonal = c(2, 1, 0)),
    arima(ts_data, order = c(1, 1, 2), seasonal = c(0, 1, 1)),
    arima(ts_data, order = c(1, 1, 2), seasonal = c(1, 1, 1)),
    arima(ts_data, order = c(1, 1, 2), seasonal = c(2, 1, 1)),
    arima(ts_data, order = c(1, 1, 3), seasonal = c(0, 1, 0)),
    arima(ts_data, order = c(1, 1, 3), seasonal = c(1, 1, 0)),
    arima(ts_data, order = c(1, 1, 3), seasonal = c(2, 1, 0)),
    arima(ts_data, order = c(1, 1, 3), seasonal = c(0, 1, 1)),
    arima(ts_data, order = c(1, 1, 3), seasonal = c(1, 1, 1)),
    arima(ts_data, order = c(1, 1, 3), seasonal = c(2, 1, 1))
)

model_comparison <- lapply(models, AIC)
best_model_index <- which.min(model_comparison)
best_model <- models[[best_model_index]]
```

Acknowledgements
Not applicable.

Author contributions
WD: Conceptualization, Methodology, Software, Writing original draft. ZF: Supervision, Review and editing. YZ: Supervision, Review and editing. All authors read and approved the final manuscript.

Funding
Z.F. acknowledge support from Guangdong Basic and Applied Basic Research Foundation (2023A1515010884).

Data availability
Data will be made available upon request.

Code availability
Not applicable.

Declarations

Ethics approval and consent to participate
Not applicable.

Consent for publication
Not applicable.

Competing interests
The authors declare no competing interests.

Author details
[1]School of Mathematics, Harbin Institute of Technology, Harbin, 150001, China. [2]School of Science, Harbin Institute of Technology, Shenzhen, 518055, China.

Received: 12 November 2024 Accepted: 2 January 2025 Published online: 31 January 2025

References

1. Atangana, A., İğret Araz, S.: Modeling and forecasting the spread of covid-19 with stochastic and deterministic approaches: Africa and Europe. Adv. Differ. Equ. **2021**, 57 (2021)
2. Ibrahim, R.W., Altulea, D., Elobaid, R.M.: Dynamical system of the growth of covid-19 with controller. Adv. Differ. Equ. **2021**, 9 (2021)
3. Bi, Q., Wu, Y., Mei, S., Ye, C., Zou, X., Zhang, Z., Liu, X., Wei, L., Truelove, S.A., Zhang, T., et al.: Epidemiology and transmission of covid-19 in 391 cases and 1286 of their close contacts in Shenzhen, China: a retrospective cohort study. Lancet Infect. Dis. **20**(8), 911–919 (2020)

4. Ciotti, M., Ciccozzi, M., Terrinoni, A., Jiang, W.-C., Wang, C.-B., Bernardini, S.: The covid-19 pandemic. Crit. Rev. Clin. Lab. Sci. **57**(6), 365–388 (2020)
5. Deng, Y., He, D., Zhao, Y.: The impacts of anti-protective awareness and protective awareness programs on covid-19 outbreaks. Chaos Solitons Fractals **180**, 114493 (2024)
6. Perra, N.: Non-pharmaceutical interventions during the covid-19 pandemic: a review. Phys. Rep. **913**, 1–52 (2021)
7. Cowling, B.J., Ali, S.T., Ng, T.W., Tsang, T.K., Li, J.C., Fong, M.W., Liao, Q., Kwan, M.Y., Lee, S.L., Chiu, S.S., et al.: Impact assessment of non-pharmaceutical interventions against coronavirus disease 2019 and influenza in Hong Kong: an observational study. Lancet Public Health **5**(5), 279–288 (2020)
8. Rezapour, S., Mohammadi, H.: A study on the ah1n1/09 influenza transmission model with the fractional Caputo–Fabrizio derivative. Adv. Differ. Equ. **2020**, 488 (2020)
9. He, D., Lin, L., Artzy-Randrup, Y., Demirhan, H., Cowling, B.J., Stone, L.: Resolving the enigma of Iquitos and Manaus: a modeling analysis of multiple covid-19 epidemic waves in two Amazonian cities. Proc. Natl. Acad. Sci. **120**(10), 2211422120 (2023)
10. Nypaver, C., Dehlinger, C., Carter, C.: Influenza and influenza vaccine: a review. J. Midwifery Women's Health **66**(1), 45–53 (2021)
11. Fröbert, O., Götberg, M., Erlinge, D., Akhtar, Z., Christiansen, E.H., MacIntyre, C.R., Oldroyd, K.G., Motovska, Z., Erglis, A., Moer, R., et al.: Influenza vaccination after myocardial infarction: a randomized, double-blind, placebo-controlled, multicenter trial. Circulation **144**(18), 1476–1484 (2021)
12. Santana-Cibrian, M., Acuna-Zegarra, M.A., Velasco-Hernandez, J.X.: Lifting mobility restrictions and the effect of superspreading events on the short-term dynamics of covid-19. Math. Biosci. Eng. **17**(5), 6240–6258 (2020)
13. Deng, Y., Lin, H., He, D., Zhao, Y.: Trending on the use of Google mobility data in covid-19 mathematical models. Adv. Cont. Discr. Mod. **2024**(1), 21 (2024)
14. Palumbo, D., Lattanzio, S., et al.: Lifting restrictions with changing mobility and the importance of soft containment measures: a seird model of covid-19 dynamics. Covid Economics **18** (2020)
15. Monge, S., Zamalloa, P.L., Moros, M.J.S., Olaso, O.P., San Miguel, L.G., Varela, C., Ariza, S.R., Torres, M.C.V., Lucerón, M.d.C.O., Yuste, P.G., et al.: Lifting covid-19 mitigation measures in Spain (May–June 2020). Enfermedades Infecciosas y Microbiologia Clinica (English ed.) **41**(1), 11–17 (2023)
16. Solomon, D.A., Sherman, A.C., Kanjilal, S.: Influenza in the covid-19 era. JAMA **324**(13), 1342–1343 (2020)
17. Dhanasekaran, V., Sullivan, S., Edwards, K.M., Xie, R., Khvorov, A., Valkenburg, S.A., Cowling, B.J., Barr, I.G.: Human seasonal influenza under covid-19 and the potential consequences of influenza lineage elimination. Nat. Commun. **13**(1), 1721 (2022)
18. Guan, W.-J., Liang, W.-H., Shi, Y., Gan, L.-X., Wang, H.-B., He, J.-X., Zhong, N.-S.: Chronic respiratory diseases and the outcomes of covid-19: a nationwide retrospective cohort study of 39,420 cases. J. Allergy Clin. Immunol. **9**(7), 2645–2655 (2021)
19. Zhou, J., Ye, Y., Arenas, A., Gómez, S., Zhao, Y.: Pattern formation and bifurcation analysis of delay induced fractional-order epidemic spreading on networks. Chaos Solitons Fractals **174**, 113805 (2023)
20. Chiner-Vives, E., Cordovilla-Perez, R., Rosa-Carrillo, D., Garcia-Clemente, M., Izquierdo-Alonso, J.L., Otero-Candelera, R., Perez-de Llano, L., Sellares-Torres, J., Granda-Orive, J.I.: Short and long-term impact of covid-19 infection on previous respiratory diseases. Arch. Bronconeumol. **58**, 39–50 (2022)
21. Olsen, S.J.: Changes in influenza and other respiratory virus activity during the covid-19 pandemic—United States, 2020–2021. Morb. Mort. Wkly. Rep. **70** (2021)
22. Feng, L., Zhang, T., Wang, Q., Xie, Y., Peng, Z., Zheng, J., Qin, Y., Zhang, M., Lai, S., Wang, D., et al.: Impact of covid-19 outbreaks and interventions on influenza in China and the United States. Nat. Commun. **12**(1), 3249 (2021)
23. Ozaras, R., Cirpin, R., Duran, A., Duman, H., Arslan, O., Bakcan, Y., Kaya, M., Mutlu, H., Isayeva, L., Kebanlı, F., et al.: Influenza and covid-19 coinfection: report of six cases and review of the literature. J. Med. Virol. **92**(11), 2657–2665 (2020)
24. Ali, S.T., Lau, Y.C., Shan, S., Ryu, S., Du, Z., Wang, L., Xu, X.-K., Chen, D., Xiong, J., Tae, J., et al.: Prediction of upcoming global infection burden of influenza seasons after relaxation of public health and social measures during the covid-19 pandemic: a modelling study. Lancet Glob. Health **10**(11), 1612–1622 (2022)
25. Ye, Y., Zhou, J., Zhao, Y.: Pattern formation in reaction-diffusion information propagation model on multiplex simplicial complexes. Inf. Sci. **689**, 121445 (2025). https://doi.org/10.1016/j.ins.2024.121445
26. Wang, Y., Zhao, Y.: Synchronization of directed higher-order networks via pinning control. Chaos Solitons Fractals **185**, 115062 (2024). https://doi.org/10.1016/j.chaos.2024.115062
27. Hu, X., Wang, Z., Sun, Q., Chen, J., Zhao, D., Xia, C.: Coupled propagation between one communicable disease and related two types of information on multiplex networks with simplicial complexes. Phys. A, Stat. Mech. Appl. **645**, 129832 (2024)
28. Burki, T.K.: Lifting of covid-19 restrictions in the UK and the Delta variant. Lancet Respir. Med. **9**(8), 85 (2021)
29. Dave, D., Friedson, A.I., Matsuzawa, K., McNichols, D., Sabia, J.J.: Sudden lockdown repeals, social mobility, and covid-19: Evidence from a judicial natural experiment. J. Empir. Leg. Stud. (2023)
30. Kapoor, N.R., Aryal, A., Mehata, S., Dulal, M., Kruk, M.E., Bauhoff, S., Arsenault, C.: Effect of lifting covid-19 restrictions on utilisation of primary care services in Nepal: a difference-in-differences analysis. BMJ Open **12**(11), 061849 (2022)
31. Li, Q., Guan, X., Wu, P., Wang, X., Zhou, L., Tong, Y., Ren, R., Leung, K.S., Lau, E.H., Wong, J.Y., et al.: Early transmission dynamics in Wuhan, China, of novel coronavirus–infected pneumonia. N. Engl. J. Med. **382**(13), 1199–1207 (2020)
32. Loo, K.-Y., Thye, A.Y.-K., Law, L.N.-S., Law, J.W.F.: Covid-19: an updated situation from Singapore. Progress in Microbes & Molecular Biology **4**(1) (2021)
33. Chinese National Influenza Center: Influenza Virus Data and Information. Chinese National Influenza Center. https://ivdc.chinacdc.cn/cnic/ (Accessed: February 8, 2024)
34. Centers for Disease Control and Prevention: Weekly Flu Surveillance Reports. CDC. https://www.cdc.gov/flu/weekly/pastreports.htm (Accessed: February 8, 2024)
35. Ministry of Health Singapore: Infectious Disease Statistics for 2022. Ministry of Health Singapore. https://www.moh.gov.sg/resources-statistics/infectious-disease-statistics/2022 (Accessed: February 8, 2024)
36. UK Health Security Agency: UKHSA data dashboard. https://ukhsa-dashboard.data.gov.uk/. Accessed: 2024-07-19

37. World Health Organization: FluNet - Global Influenza Surveillance and Response System. World Health Organization. https://www.who.int/tools/flunet (Accessed: February 8, 2024)
38. Soo, R.J.J., Chiew, C.J., Ma, S., Pung, R., Lee, V.: Decreased influenza incidence under covid-19 control measures, Singapore. Emerg. Infect. Dis. **26**(8), 1933 (2020)
39. Our World in Data: Biweekly Confirmed COVID-19 Cases. Our World in Data. https://ourworldindata.org/grapher/biweekly-confirmed-covid-19-cases (Accessed: February 8, 2024)
40. Guerra, F.M., Bolotin, S., Lim, G., Heffernan, J., Deeks, S.L., Li, Y., Crowcroft, N.S.: The basic reproduction number (r0) of measles: a systematic review. Lancet Infect. Dis. **17**(12), 420–428 (2017)
41. Cori, A., Ferguson, N.M., Fraser, C., Cauchemez, S.: A new framework and software to estimate time-varying reproduction numbers during epidemics. Am. J. Epidemiol. **178**(9), 1505–1512 (2013)
42. Gostic, K.M., McGough, L., Baskerville, E.B., Abbott, S., Joshi, K., Tedijanto, C., Kahn, R., Niehus, R., Hay, J.A., De Salazar, P.M., et al.: Practical considerations for measuring the effective reproductive number, r t. PLoS Comput. Biol. **16**(12), 1008409 (2020)
43. Griffin, J., Casey, M., Collins, Á., Hunt, K., McEvoy, D., Byrne, A., McAloon, C., Barber, A., Lane, E.A., More, S.: Rapid review of available evidence on the serial interval and generation time of covid-19. BMJ Open **10**(11), 040263 (2020)
44. Knight, J., Mishra, S.: Estimating effective reproduction number using generation time versus serial interval, with application to covid-19 in the greater Toronto area, Canada. Infect. Dis. Model. **5**, 889–896 (2020)
45. Musa, S.S., Zhao, S., Wang, M.H., Habib, A.G., Mustapha, U.T., He, D.: Estimation of exponential growth rate and basic reproduction number of the coronavirus disease 2019 (covid-19) in Africa. Infect. Dis. Poverty **9**(1), 1–6 (2020)
46. Backer, J.A., Eggink, D., Andeweg, S.P., Veldhuijzen, I.K., Maarseveen, N., Vermaas, K., Vlaemynck, B., Schepers, R., Hof, S., Reusken, C.B., et al.: Shorter serial intervals in sars-cov-2 cases with omicron ba. 1 variant compared with delta variant, the Netherlands, 13 to 26 December 2021. Euro Surveill. **27**(6), 2200042 (2022)
47. Nikbakht, R., Baneshi, M.R., Bahrampour, A., Hosseinnataj, A.: Comparison of methods to estimate basic reproduction number (r0) of influenza, using Canada 2009 and 2017-18 a (h1n1) data. J. Res. Med. Sci. **24** (2019)
48. Ospina, R., Gondim, J.A., Leiva, V., Castro, C.: An overview of forecast analysis with arima models during the covid-19 pandemic: methodology and case study in Brazil. Mathematics **11**(14), 3069 (2023)
49. Alabdulrazzaq, H., Alenezi, M.N., Rawajfih, Y., Alghannam, B.A., Al-Hassan, A.A., Al-Anzi, F.S.: On the accuracy of arima based prediction of covid-19 spread. Results Phys. **27**, 104509 (2021)
50. Sahai, A.K., Rath, N., Sood, V., Singh, M.P.: Arima modelling & forecasting of covid-19 in top five affected countries. Diabetes Metab. Syndr. Clin. Res. Rev. **14**(5), 1419–1427 (2020)
51. California Department of Public Health: Title of the Webpage. https://www.cdph.ca.gov/Programs/OPA/Pages/NR21-214.aspx. Accessed: 2024-07-19 (2021)
52. California Department of Public Health: Title of the Webpage. https://www.cdph.ca.gov/Programs/OPA/Pages/NR21-234.aspx. Accessed: 2024-07-19 (2021)
53. Ministry of Health Singapore: Focusing Our Resources and Refining Our Healthcare Protocols to Deal with the Omicron Wave. https://www.moh.gov.sg/news-highlights/details/focusing-our-resources-and-refining-our-healthcare-protocols-to-deal-with-the-omicron-wave. Accessed: 2024-07-19
54. Ministry of Health Singapore: Rise in BA.4 and BA.5 subvariant cases drives recent increase in COVID-19 cases. https://www.moh.gov.sg/news-highlights/details/rise-in-ba.4-and-ba.5-subvariant-cases-drives-recent-increase-in-covid-19-cases. Accessed: 2024-07-19
55. Ministry of Health Singapore: Extension of Safe Management Measures for in-Person Visits to Hospitals and Residential Care Homes. https://www.moh.gov.sg/news-highlights/details/extension-of-safe-management-measures-for-in-person-visits-to-hospitals-and-residential-care-homes-9nov22. Accessed: 2024-07-19 (2022)

Publisher's Note